Liquid Crystals
Publication details, including instructions for authors and subscription information:
http://www.informaworld.com/smpp/title~content=t713926090

Nematic liquid crystals in frequency and amplitude modulated electric fields

B. I. Lev; V. N. Sergienko; P. M. Tomchuk; E. K. Frolova

Online publication date: 06 August 2010

To cite this Article Lev, B. I. , Sergienko, V. N. , Tomchuk, P. M. and Frolova, E. K.(2001) 'Nematic liquid crystals in frequency and amplitude modulated electric fields', Liquid Crystals, 28: 7, 973 — 982
To link to this Article: DOI: 10.1080/02678290110048282
URL: http://dx.doi.org/10.1080/02678290110048282

LIQUID CRYSTALS, 2001, VOL. 28, NO. 7, 973–982

Nematic liquid crystals in frequency and amplitude modulated electric fields

B. I. LEV, V. N. SERGIENKO*, P. M. TOMCHUK and E. K. FROLOVA
Institute of Physics, prosp. Nauki 46, Kiev 03028, Ukraine

(*Received 10 May 2000; in final form 1 September 2000; accepted 19 September 2000*)

In this paper we study peculiarities of behaviour of a nematic liquid crystal (NLC) in an electric field consisting of two harmonics with different amplitudes and frequencies. The most interesting result is the experimental observation of high frequency, stabilization of a low frequency electrohydrodynamic instability in the NLC. A method of measurement of the one frequency instability threshold has been proposed. The beating regime of the two frequency electric field was also studied. The theory developed provides an explanation for all the experimental results.

1. Introduction

It is well known that under a relatively low power electric or magnetic field, the initial director distribution of a nematic liquid crystal (NLC) can become unstable. The loss of stability brings about charge and director flows and consequently transitional structures and new steady states can occur. Electrohydrodyna mic instabilities of a NLC are the most intensively studied [1–7]. Traditionally, investigation of such instabilities is carried out by applying a d.c. or a.c. electric field. Depending on the mesophase parameters (anisotropy of permittivity, conductivity, viscosity) various structures appear in different frequency ranges: Williams domains, chevrons, cell-type structures, etc. In view of the fact that the liquid crystal response to an external field is non-linear, it is likely that an electric field of more complicated (than sinusoidal) temporal behaviour might give rise to new structures, as well as modify the properties of the known ones. The simplest form of a non-sinusoidal field is a superposition of two harmonic waves with the same amplitudes. The first studies of NLC under such a field were initiated in refs [8, 9]. This paper concerns a closer theoretical and experimental examination of the behaviour of a NLC in a biharmonic electric field in the case where both amplitudes, as well as both frequencies, are distinct.

One of the most interesting results is the experimental observation of a high frequency stabilization of a low frequency electrohydrodynamic instability in the NLC. This stabilization takes place for certain combinations of amplitudes whose absolute values are connected with both applied frequencies. Extrapolation of the dependence to zero amplitude of one frequency allows the threshold voltage to be found more reliably and readily than by standard procedures. First we shall consider the theory and then the experimental results finally we discuss the agreement between theory and experiment.

*Author for correspondence; e-mail: turchin@iop.kiev.ua

2. Theory

The behaviour of a NLC in an electric field is given by the well known equations [1–4]:

$$\begin{aligned} \dot{q} + \omega_c q + \sigma_H E\Psi = 0 \\ \dot{\Psi} + \omega_0 \Psi + \lambda E^2 \Psi + \mu E q = 0 \end{aligned} \tag{1}$$

where q is the electrical charge density, $\Psi = \partial\Theta/\partial x$ is the director curvature, Θ is the angle between the director and the x-axis which lies in the plane of the cell;

$$\omega_c = \frac{4\pi\sigma_\parallel}{\varepsilon_\parallel}, \quad \omega_0 = \frac{\eta_c}{\gamma_1 \tilde{\eta}_c} K_{33} k^2$$

are the frequencies of the charge and director decay, respectively;

$$\sigma_H = \left(\frac{\varepsilon_\perp}{\varepsilon_\parallel} - \frac{\sigma_\perp}{\sigma_\parallel}\right)\sigma_\parallel; \quad \mu = \frac{\eta_c}{\gamma_1 \tilde{\eta}_c}\left(\frac{\varepsilon_\perp - \varepsilon_\parallel}{\varepsilon_\parallel} - \frac{\alpha_2}{\eta_c}\right),$$

$$\lambda = \frac{\eta_c}{\gamma_1 \tilde{\eta}_c} \frac{\varepsilon_\perp - \varepsilon_\parallel}{4\pi\varepsilon_\parallel}\varepsilon_\perp$$

where $\sigma_\parallel$, $\sigma_\perp$ are the longitudinal and transverse components of the conductivity tensor, $\varepsilon_\parallel$, $\varepsilon_\perp$ are those of the permittivity tensor, α_2 and γ_1 are Leslie coefficients, η_c and $\tilde{\eta}_c$ are the effective coefficients of viscosity [1–4]; K_{33} is the bend elastic constant, and k is the wave number which is inversely proportional to the cell thickness d. The dots over q and Ψ stand for the time derivative.

Liquid Crystals ISSN 0267-8292 print/ISSN 1366-5855 online © 2001 Taylor & Francis Ltd
http://www.tandf.co.uk/journals
DOI: 10.1080/02678290110048282

According to the experimental conditions, the biharmonic electric field directed along the z-axis normal to the cell is of the form

$$E = E_1 \cos \omega_1 t + E_2 \cos \omega_2 t = 2E_0 \cos \omega t \cos \Delta\omega t + 2\Delta E \sin \omega t \sin \Delta\omega t \quad (2)$$

where

$$E_0 = 1/2(E_1 + E_2), \quad \Delta E = 1/2(E_1 - E_2),$$
$$\omega = 1/2(\omega_1 + \omega_2), \quad \Delta\omega = 1/2(\omega_1 - \omega_2).$$

To describe the dynamics of the NLC we introduce fast and slow variables of q and Ψ. Let $q = \bar{q} + \delta q$ and $\Psi = \bar{\Psi} + \delta\Psi$ where $\bar{q}$ and $\bar{\Psi}$ describe long time mean values of the charge and director curvature, respectively, while δq and $\delta\Psi$ are their fast changes. Substituting such representations into equation (1) and performing the time averaging we obtain the following equations:

$$\begin{aligned} \ddot{\bar{q}} + \omega_c \dot{\bar{q}} + \sigma_H \overline{E\delta\Psi} = 0 \\ \dot{\bar{\Psi}} + \omega_0 \bar{\Psi} + \lambda \overline{E^2 \Psi} + \overline{\mu E \delta q} = 0. \end{aligned} \quad (3)$$

By subtracting the corresponding equations of system (3) from those of sytem (1), one obtains the following equations for the fast variables:

$$\begin{aligned} \dot{\delta q} + \omega_c \delta q + \sigma_H E \bar{\Psi} = 0 \\ \delta\dot{\Psi} + \omega_0 \delta\Psi + \lambda \overline{E^2} \delta\Psi + \mu E \bar{q} = 0. \end{aligned} \quad (4)$$

In equations (3) and (4), only the terms which contain lower harmonics of ω and $\Delta\omega$ were retained.

The averaging procedure strongly depends on the relation between the frequencies of the applied field and the relaxation times of the charge and director. We will consider different cases separately.

2.1. *Field frequencies differ widely*

When the frequencies differ considerably, ($\omega_2 \gg \omega_1$, and $\omega_2 > \omega_c, \omega_0$), the time averaging may be performed over intervals obeying the inequality $\Delta\omega T \gg 1$. In this situation, the behaviour of the mesophase is described by a flow variation of $\bar{q}$ and $\bar{\Psi}$ for time, significantly longer than the time of averaging. To seek the solution of equations (4) for the fast variables, the temporal dependence of the electric field E in an explicit form must be taken into account. Thus we can take δq and $\delta\Psi$ in the form:

$$\begin{Bmatrix} \delta q \\ \delta\Psi \end{Bmatrix} = \begin{Bmatrix} a_1 \\ b_1 \end{Bmatrix} \sin \omega t \sin \Delta\omega t + \begin{Bmatrix} a_2 \\ b_2 \end{Bmatrix} \sin \omega t \cos \Delta\omega t + \begin{Bmatrix} a_3 \\ b_3 \end{Bmatrix} \cos \omega t \sin \Delta\omega t + \begin{Bmatrix} a_4 \\ b_4 \end{Bmatrix} \cos \omega t \cos \Delta\omega t. \quad (5)$$

The upper coefficients a_i refer to δq, while the lower ones b_i refer to $\delta\Psi$. Substituting equation (5) into (4) and setting equal the coefficients of similar combinations of envelope functions, we obtain the system of algebraic equations for coefficients a_i and b_i. Thus, for example, we have:

$$\begin{aligned} a_1 &= -2\sigma_H \bar{\Psi} \omega_c \frac{2E_0 \Delta\omega\omega + \Delta E(\omega^2 + \Delta\omega^2 + \omega_c^2)}{(\omega^2 + \Delta\omega^2 + \omega_c^2) - 4\Delta\omega^2\omega^2} \\ b_4 &= -2\mu\bar{q}\omega_d \frac{E_0(\omega^2 + \Delta\omega^2 + \omega_d^2) + 2\Delta E\Delta\omega\omega}{(\omega^2 + \Delta\omega^2 + \omega_d^2) - 4\Delta\omega^2\omega^2} \end{aligned} \quad (6)$$

where $\omega_d \equiv \omega_0 + \lambda(E_0^2 + \Delta E^2)$. Similar expressions can be obtained for the other coefficients.

Averaging over the characteristic time of the fast variables gives:

$$\bar{E}^2 = \lim_{T\to\infty} \frac{1}{T} \int_0^T dt(2E_0 \cos \omega t \cos \Delta\omega t + 2\Delta E \sin \omega t \sin \Delta\omega t)^2 = E_0^2 + \Delta E^2 \quad (7)$$

and

$$\overline{E\delta q} = (E_0 a_4 - \Delta E a_1)/2, \quad \overline{E\delta\Psi}. \quad (8)$$

By using equation (8) and explicit expressions for the time-dependent coefficients (6), we obtain a simple equation for $\bar{\Psi}$ and $\bar{q}$ alone:

$$\partial\bar{\Psi}/\partial t + \gamma_d \bar{\Psi} = 0, \quad \partial\bar{q}/\partial t + \gamma_q \bar{q} = 0 \quad (9)$$

where

$$\gamma_d = \omega_d - \frac{\mu\sigma_H\omega_c[(E_0^2 + \Delta E^2)(\omega^2 + \Delta\omega^2 + \omega_c^2) + 4\Delta E E_0 \Delta\omega\omega]}{(\omega^2 + \Delta\omega^2 + \omega_c^2)^2 - 4\Delta\omega^2\omega^2} \quad (10)$$

$$\gamma_q = \omega_c - \frac{\mu\sigma_H\omega_d[(E_0^2 + \Delta E^2)(\omega^2 + \Delta\omega^2 + \omega_d^2) + 4\Delta E E_0 \Delta\omega\omega]}{(\omega^2 + \Delta\omega^2 + \omega_d^2)^2 - 4\Delta\omega^2\omega^2}. \quad (11)$$

It is seen from equations (9) that for a large difference of frequencies, the equation for the slow components of the director and charge become independent. The solutions of these equations can be expressed as $\bar{\Psi} \sim \exp(-\gamma_d t)$, $\bar{q} \sim \exp(-\gamma_q t)$.

Conditions for initiation of the instabilities are obtained by setting the corresponding decay decrement equal to zero. In such a way, one can find a functional

dependence between E_1, E_2, ω_1, and ω_2. For example, Williams domains (conductivity regime, $\gamma_d = 0$) occur for

$$(\omega_2^2 + \omega_c^2)[\xi^2\omega_c^2 - (\omega_1^2 + \omega_c^2)]E_1^2 + (\omega_1^2 + \omega_c^2)\xi^2\omega = \frac{2\omega_0}{\lambda}(\omega_1^2 + \omega_c^2)(\omega_2^2 + \omega_c^2) \quad (12)$$

where the parameter

$$\xi^2 = \frac{\mu\sigma_H}{\lambda\omega_c} = \left(1 - \frac{\sigma_\perp \varepsilon_\parallel}{\sigma_\parallel \varepsilon_\perp}\right)\left(1 + \frac{\alpha_2 \varepsilon_\parallel}{\eta_2(\varepsilon_\parallel - \varepsilon_\perp)}\right) \quad (13)$$

has the well known form (equation (12) can also be written for the dielectric regime if ω_c is replaced by ω_d). Assuming $E_1 = E_2$ it is easy to get the critical field of instability for the conductivity regime, i.e.

$$E_c^2 = \frac{2\omega_0}{\lambda}\frac{(\omega_1^2 + \omega_c^2)(\omega_2^2 + \omega_c^2)}{\xi^2\omega_c^2(\omega_1^2 + \omega_2^2 + 2\omega_c^2) - 2(\omega_1^2 + \omega_c^2)(\omega_2^2 + \omega_c^2)}. \quad (14)$$

The critical frequency for the dielectric regime can be obtained from the condition $\gamma_d = 0$. Setting $\omega_d \cong \lambda E_0^2$ this condition has the form

$$\omega_d^2 = -\frac{\xi^2 - 2}{2(\xi^2 - 1)}(\omega^2 + \Delta\omega^2) \times \left\{1 \pm \left[1 + \frac{4(\xi^2 - 1)(\omega^2 - \Delta\omega^2)^2}{(\xi^2 - 2)(\omega^2 + \Delta\omega^2)^2}\right]^{1/2}\right\}. \quad (15)$$

If $\omega_d^2 \geqslant 0$, we must take the minus sign before the square root in equation (15) for $\xi^2 > 2$, and the plus sign for $2 > \xi^2 > 1$. If $\Delta\omega \simeq \omega$, that is $\omega_2 \gg \omega_1$, the following approximate relation for ω_d exists

$$\omega_d^2 = \frac{2\omega_1^2\omega_2^2}{(\xi^2 - 2)(\omega_1^2 + \omega_2^2)} \simeq \frac{2\omega_1^2}{(\xi^2 - 2)}$$

while the critical electric field can be written as

$$E_c = \left(\frac{\omega_d}{\lambda}\right)^{1/2} = \left[\frac{\omega_1}{\lambda(\xi^2 - 2)^{1/2}}\right]^{1/2} \quad (16)$$

Consequently, the threshold field is proportional to $\omega_1^{1/2}$. As soon as the denominator in equation (14) vanishes, transition from the conductive to the dielectric regime takes place. The frequency of this transition is defined by

$$\omega_2^2 = \omega_k^2 = \omega_c^2\left\{\frac{\xi^2(\omega_1^2 + \omega_c^2)}{2(\omega_1^2 + \omega_c^2) - \xi^2\omega_c^2} - 1\right\}. \quad (17)$$

Equation (17) is valid only if the expression in the curly brackets is positive since only in this case is a real value of ω_2 obtained and thus the transition is possible. If the lower frequency ω_1 satisfies the inequality $\omega_1 < \omega_c(\xi^2/2 - 1)^{1/2}$ then switching to the dielectric regime does not occur. For $\xi^2 > 2(1 + \omega_1^2/\omega_c^2)$, the critical field is independent of the higher frequency and tends to a constant value $E_c^2 = 2\omega_0^2/\lambda(\xi^2 - 2)$.

2.2. *Field frequencies are similar*

Now let us consider the beating regime when the frequencies of the applied fields are not too different from one another, that is $\Delta\omega \ll \omega_1, \omega_2$. In this case, the averaging procedure for the field can be written as

$$\overline{E^2} = \frac{1}{T}\int_0^T E(t)\,dt = 2E_0^2\cos^2\Delta\omega t + 2\Delta E^2\sin^2\Delta\omega t. \quad (18)$$

Expressing

$$\delta q = A_1\cos\omega t + A_2\sin\omega t \quad \text{and}$$
$$\delta\Psi = B_1\cos\omega t + B_2\sin\omega t$$

from the equations of system (4) and substituting them into (3) we can obtain the equations for $\bar{q}$ and $\bar{\Psi}$. Since in the experiment the director (which is the slow subsystem) is studied it will be sufficient to consider the equation only for $\bar{\Psi}$, i.e.

$$\dot{\bar{\Psi}} + \left[\omega_0 + \lambda\left(1 - \frac{\xi^2\omega_c^2}{\omega_c^2 + \omega^2}\right)(E_0^2 + \Delta E^2) + \lambda\left(1 - \frac{\xi^2\omega_c^2}{\omega_c^2 + \omega^2}\right)(E_0^2 - \Delta E^2)\cos 2\Delta\omega t\right]\bar{\Psi} = 0. \quad (19)$$

This has the solution

$$\bar{\Psi} = const\exp\left[-\gamma t - \frac{\gamma(E_0^2 - \Delta E^2)}{2\Delta\omega(E_0^2 + \Delta E^2)}\sin 2\Delta\omega t\right] \quad (20)$$

where

$$\gamma = \omega_0 + \lambda\left(1 - \frac{\xi^2\omega_c^2}{\omega_c^2 + \omega^2}\right)(E_0^2 + \Delta E^2). \quad (21)$$

Solution (20) implies an exponential growth of $\bar{\Psi}$ for $\gamma < 0$, that is the onset of the instability. Its critical field is determined from the condition $\gamma = 0$. For fields with equal amplitudes ($\Delta E = 0$) the critical voltage is

$$E_{0c}^2 = \frac{\omega_0(\omega_c^2 + \omega^2)}{\lambda[\xi^2\omega_c^2 - (\omega_c^2 + \omega^2)]} \quad (22)$$

This is a familiar result which corresponds to the threshold voltage of Williams domains for $\omega_1 = \omega_2 = \omega$.

2.3. *Pulsed field*

Here we discuss the behaviour of a NLC under a pulsed electric field. In the general case, the solution of

the first equation of system (1) can be written in the form

$$q = -\sigma_H \int_{-\infty}^{0} E(s+t)\Psi(s+t)\exp(\omega_c s)\,ds \quad (23)$$

where $q = 0$ for $t = -\infty$. Substituting this solution into the second equation of system (1) we obtain a closed equation that describes the behaviour of the slow sub-system in the form

$$\dot{\Psi} + \omega_0\Psi + \lambda E^2(t)\Psi - \mu\sigma_H E(t) \times \int_{-\infty}^{0} E(s+t)\Psi(s+t)\exp(\omega_c s)\,ds = 0. \quad (24)$$

Using the notation $F(t) = E(t)\Psi(t)$ and integrating by parts we obtain an equation with memory:

$$\dot{\Psi} + [\omega_0 + \lambda(1-\xi^2)E^2(t)]\Psi + \xi^2\lambda E(t)\int_{-\infty}^{0} \frac{dF(s+t)}{ds}\exp(\omega_c s)\,ds = 0. \quad (25)$$

However it is not possible to get a general solution of the last equation in an analytical form. For the field of type

$$E(t) = \begin{cases} E_1, & n(T_1+T_2) \leqslant t < (n+1)T_1 + nT_2 \\ E_2, & (n+1)T_1 + nT_2 \leqslant t < (n+1)(T_1+T_2) \end{cases} \quad (26)$$

(two periodic rectangular pulses with durations T_1 and T_2 and amplitudes E_1 and E_2) the memory effects can be neglected, when $T_1\omega_c,\ T_2\omega_c > 1$, and equation (25) has the solution

$$\Psi_n = \Psi_0 \exp[-\omega_0 n(T_1+T_2) + n\lambda(\xi^2-1)(E_1^2T_1 + E_2^2T_2)]. \quad (27)$$

From equation (27) it is possible to obtain a relation between E_1, E_2, T_1 and T_2 in the vicinity of the instability threshold. This can be reduced to the form

$$E_1^2 + E_2^2\frac{T_2}{T_1} = \frac{\omega_0}{\lambda(\xi^2-1)}\left(1+\frac{T_2}{T_1}\right). \quad (28)$$

When $E_2 = 0$, the instability occurs if

$$E_{1c}^2 \geqslant \frac{\omega_0}{\lambda(\xi^2-1)}\left(1+\frac{T_2}{T_1}\right) = E_c^2\left(1+\frac{T_2}{T_1}\right). \quad (29)$$

Then equation (29) yields $E_{1c} = E_c(T_2/T_1)^{1/2}$ if $T_2/T_1 > 1$, and $E_{1c} = E_c(1 + T_2/2T_1)$ if $T_2/T_1 \ll 1$.

From equations (28) and (29) it follows that $E_{1c}^2 = E_c^2$ for $T_1 \to \infty$ or $T_2 \to 0$. This corresponds to the critical field value for a stationary state. It is easy to show that if $T_1 = T_2$, the relation between E_1 and E_2 has the form

$$E_1^2 + E_2^2 = \frac{2\omega_0}{\lambda(\xi^2-1)}. \quad (30)$$

Therefore the proposed model, which contains both the charge and director sub-systems, allows us to describe the mesophase dynamics under a biharmonic electric field with different frequencies and amplitudes. From equations (14, 15, 17, 22 and 29) the threshold voltages and critical frequencies could be estimated and checked experimentally.

3. The samples and experimental technique

We studied the NLC MBBA and a mixture ZhK-440 of azobenzene derivatives with nematic mesophases from 21 to 45°C and from −5 to 75°C, respectively. The NLC was placed into a thermostabilized planar cell. The temperature of the cell was stabilized to better than ±0.1°C.

The optical liquid crystal cells were constructed from two rectangular glass plates; the distance between them was given by the polyamide insulating spacer of about 50 μm thickness. The inner surfaces of the cells were covered with transparent electrodes (indium oxide), spin-coated with a PVA alignment layer. A planar orientation of the director in such cells was obtained by rubbing and could be changed by the electric field which was normal to the surface of the cell.

The external electric field was produced by two sinusoidal voltages with different amplitudes and frequencies applied to semi-transparent contacts of the hermetically sealed cell. The form of the electric field is given in the inset of the figures. For a specific case, the amplitudes of both voltages were set equal, but their frequencies were different: one was fixed and the other was varied from 20 Hz to 100 kHz. An electric field in the form of a sequence of radio-wave pulses of different duration, frequency and amplitude was also used. The instability threshold was detected as follows. Usually in the vicinity of the threshold voltage, the electric charge and director are spatially periodic; consequently, the refractive index of the NLC also changes periodically. This suggests a means of accurate measurement of the threshold voltage as follows. We observed the diffraction pattern caused by the He-Ne laser light passing through the NLC cell. Approaching the lowest threshold voltage, only one maximum from each side of the zero order beam was observed (commonly, the most intense maxima are of the second order). This maximum indicated that a deformation of the uniform director distributions taking place. As the voltage increased, other maxima of up to 20–30 orders appeared (visual observations of the maxima on a screen, as well as by their registration using a photodetector were possible). The experimental

set-up also permitted viewing of the inhomogeneous structures of the NLC using a polarizing microscope. However, the sensitivity of such a registration of the threshold voltage was considerably lower than that by observation of the diffraction pattern.

4. Results of measurements

The difference between the behaviours of the NLC under the harmonic and biharmonic electric fields is quite drastic. In addition to well known structures that normally arise, many new structures could form in the biharmonic field (two of them are shown in figure 1). A more detailed description of these structures will be published later.

Interconversion of the structures depends on the parameters of both harmonics. Applying a biharmonic electric field with different frequencies of both components it is possible to influence the fast (charge) and slow (director) sub-systems of the medium separately. As a result, the order in which a known structure usually appears may be changed. For instance, the cell-structure can occur before the Williams domains. To investigate the problem quantitatively we have measured the dependence of the threshold voltage V_c of instability of the uniform director distribution upon higher frequency when the lower frequency is fixed. To elucidate the influence of the NLC conductivity on V_c, doped ZhK-440 was also investigated. The data obtained are presented in figure 2 for specimens ZhK-440 with and without dopant. A similar dependence was observed for MBBA (figure 3).

The results represented in figures 2 and 3 are related to the case in which the amplitudes of both harmonics are equal. All the dependences are characterized by the same properties: saturation of the threshold voltage under high frequencies and minimal threshold values for equal frequencies of the fields. Impurities, the thickness of the LC layer and its temperature change these dependences only quantitatively.

The threshold behaviour in the case of close frequencies (beating regime) was investigated in more detail taking equal amplitudes of both components of the applied field. The threshold voltage as a function of $(\omega_2 - \omega_1)^{1/2}$ is shown in figure 4 for $\omega_2 = 200$ and 297 Hz.

When the difference between frequencies is small, V_c is directly proportional to $(\omega_2 - \omega_1)^{1/2}$ and changes considerably more slowly as soon as $(\omega_2 - \omega_1) > 1$–2 Hz. Diffraction maxima accompanying the stability loss in this region appear and disappear periodically with time, the frequency being equal to the beating frequency; at some value of the latter, the pattern becomes stationary. The temporal behaviour of the diffraction picture described depends on the time which is necessary for developing and visualization of structure occurring after stability loss of the homogeneous director distribution. This was confirmed by the results obtained with radio-wave pulses of a single carrying frequency (figure 5, curves 1 and 2).

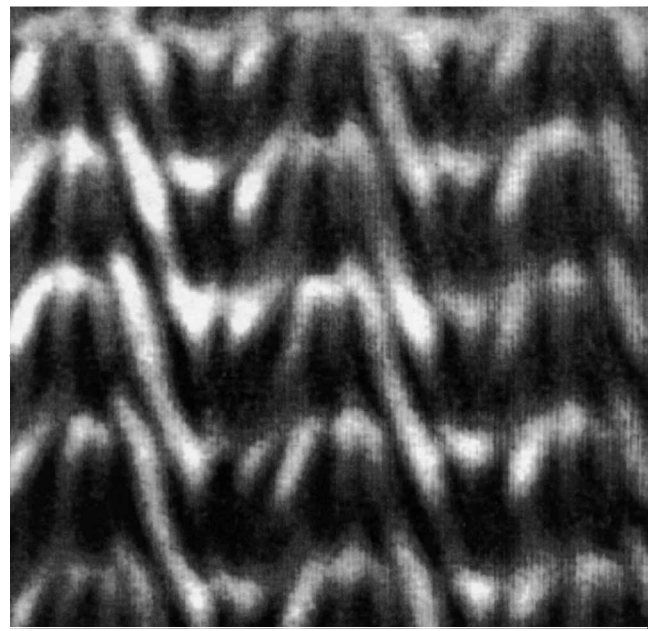

(*a*)

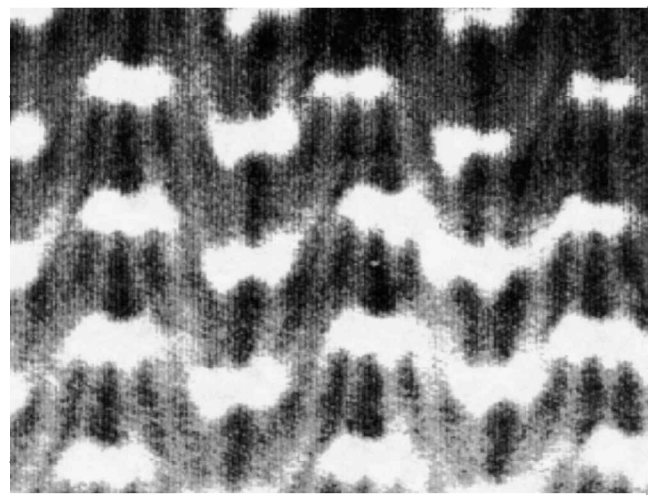

(*b*)

Figure 1. Optical patterns of ZhK-440 observed in a flat cell at room temperature in the beating regime; the carrying frequency in 300 Hz and the beat period 1 s. The maximum amplitude in (*a*) is 30 V and in (*b*) is 35 V.

In this case, a smooth amplitude growth and decrease peculiar to the beat signal (inset in figure 4) are practically absent, whereas the threshold voltage depends on both the radio-wave pulse length T_1 and the time interval T_2 between the pulses. Curve 1 in figure 5 demonstrates a very fast growth (of almost exponential type) of threshold voltage with decreasing T_1 for fixed T_2.

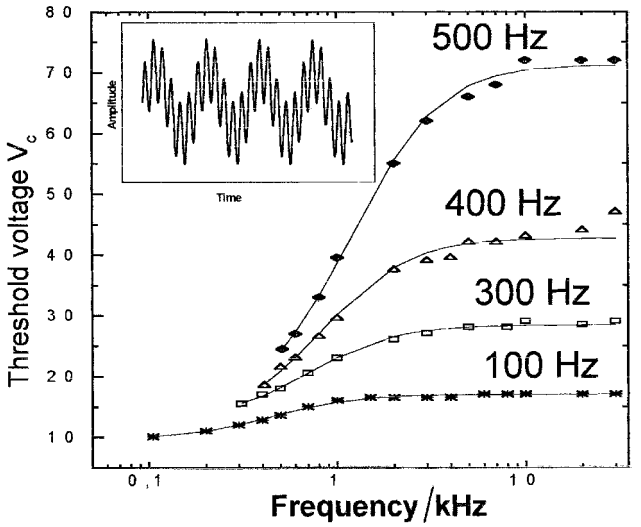

(*a*)

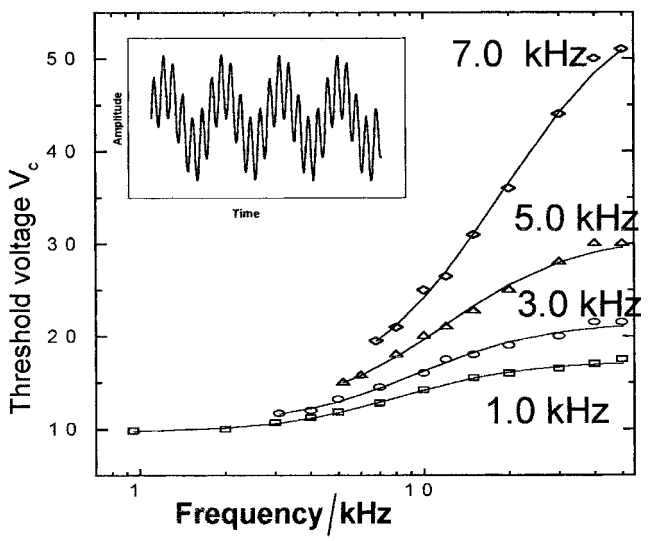

(*b*)

Figure 2. Dependence of the threshold voltage of loss of stability of the uniform director distribution on high frequency, when the low frequency is fixed for (*a*) ZhK-440 ($d = 53\,\mu m$), (*b*) doped ZhK-440 ($d = 51\,\mu m$): solid lines are for numerical values from equation (14), points are for experimental data.

Contrary to this, when T_1 is fixed ($T_1 = 0.5$ s) the threshold decreases linearly as T_2 decreases, as can be seen from curve 2. In figure 5 also, the results of measurements with radio-wave pulses with modulated carrying frequency (curves 3 and 4) are presented. It is seen that the curves have a qualitatively similar behaviour, but significant differences in the absolute values of V_c.

If the frequencies of the harmonics differ essentially (i.e. $\omega_2 - \omega_1 > \omega_1$) there is a certain functional dependence between the amplitudes of the applied voltages at

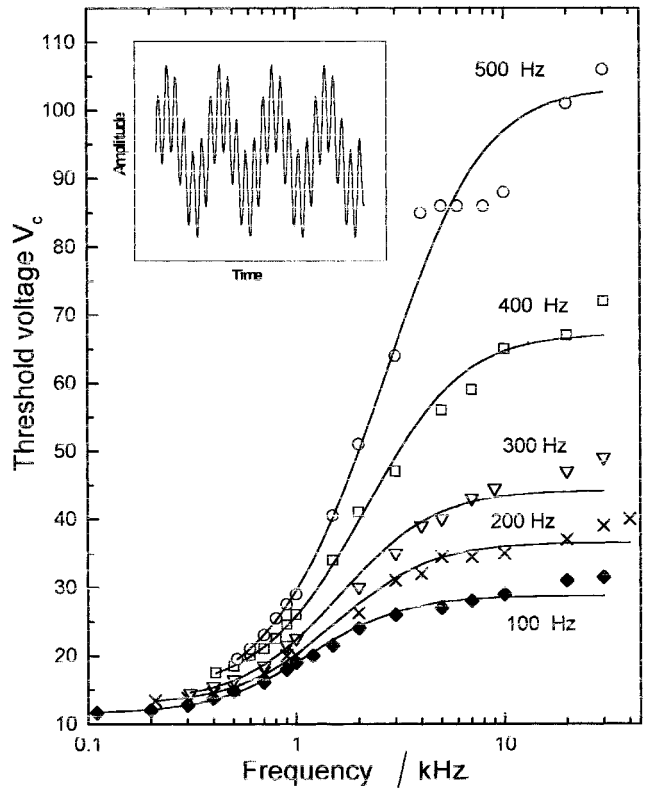

Figure 3. Same as figure 2, but for MBBA ($d = 58\,\mu m$).

which the instability arises. From figure 6 where this dependence is presented we conclude that it has a form $E_1^2 = a + bE_2^2$.

In the single frequency regime, different types of structure occur in different frequency and field ranges. In our case of a two frequency field, we were able to obtain different structures by varying solely the ratio of the amplitudes and frequencies of the harmonics of the applied voltages. A similar functional relation (figure 7) between the squares of the amplitudes was observed for the pulse regime if the filling frequencies of the pulses are the same, but the amplitudes are different.

5. Discussion

Numerical values of the threshold voltages for Williams domains in the biharmonic regime calculated from equation (14) are represented in figures 2 and 3 by solid lines, while the experimental data are shown by the points. It is evident from both the theoretical and experimental curves that the addition of a high frequency component to the slow electric field increases the threshold voltage (a minimum value of the Williams domains threshold is obtained when both frequencies are equal, that is in the single frequency regime). The same behaviour of the electric field threshold is typical for other NLC hydrodynamic instabilities. This means

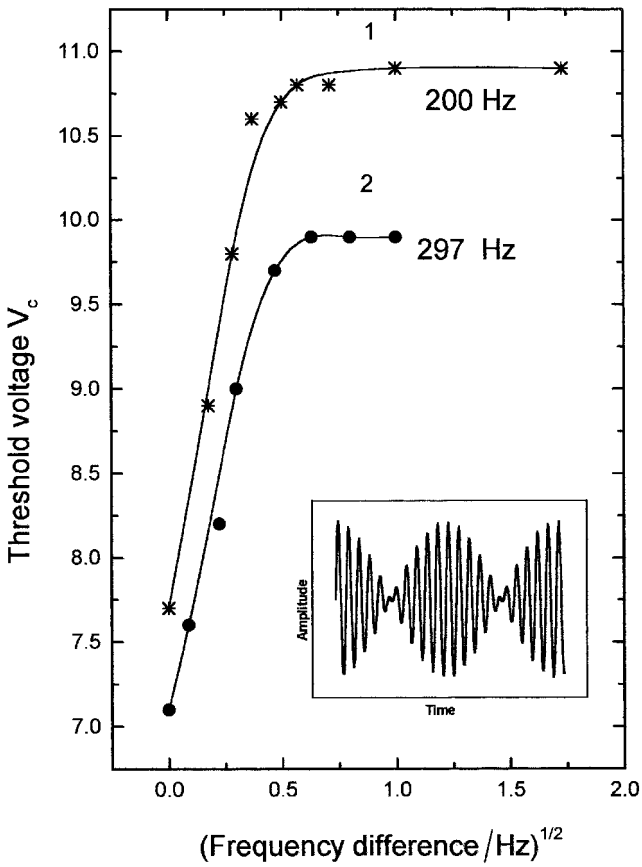

Figure 4. Threshold voltage in the beating regime versus (frequency difference)$^{1/2}$ for ZhK-440 (1) and doped ZhK-440 (2).

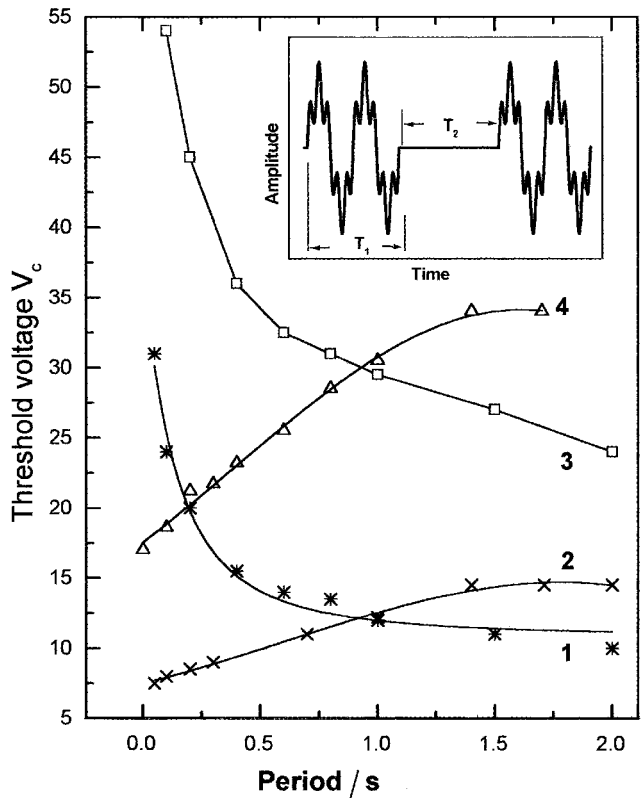

Figure 5. Threshold voltage for ZhK-440 versus impulse length T_1 for $T_2 = 1.7$ s (curves 1 and 3) and versus T_2, time between impulse (curves 2 and 4) for $T_1 = 0.5$ s: curves 1, 2 $\omega_1 = \omega_2 = 200$ Hz; curves 3, 4 $\omega_1 = 200$ Hz, $\omega_2 = 11$ kHz.

that the patterns of a NLC which become unstable in a low frequency electric field (in figures 2 and 3, this is the planar director orientation formed by the walls of a cell) can be stabilized by applying a high frequency harmonic electric field. For instance, under a harmonic electric field with frequency $\omega_1 = 200$ Hz and amplitude 25 V, the cell-type structures or dynamic scattering can be observed. Adding the other harmonic field with $\omega_2 > \omega_1$, but so that the amplitude of the biharmonic voltage remains 25 V and $E_1 = E_2$, the director patterns transform with increase in the frequency ω_2. When ω_2 approaches 1 kHz, the original planar director orientation restores. However, the stabilization of the uniform director distribution cannot be achieved for a voltage that is above the saturation range of the curves on figure 2. For instance, in the case discussed above, stabilization of the planar director orientation does not take place if the amplitude exceeds 28 V.

The behaviour discussed above is typical for equal amplitudes. If it is not the case, the threshold of the instability increases with amplitude of the high frequency component and can exceed that of the above case. As a result, stabilization of a low frequency state will also be obtained for any amplitude of the low frequency harmonic. This is illustrated by the behaviour of the Williams domains in figure 6 where experimental values of E_1^2 as a function of E_2^2 are shown for fixed ω_1 and ω_2. It is seen that E_1^2 is linear in E_2^2. The slope of the line depends on the frequencies of both components. The threshold voltage of the single frequency regime can be obtained as the intersection of this line with the ordinate axis. The threshold value determined in such a way agrees with values obtained from other measurements. By this procedure, reliable results can be obtained much more easily than for the case of the single frequency regime. This behaviour of a NLC is reminiscent of that of an unstable mechanical system in a high frequency field [10].

To make a fit between theoretical predictions and the data, the parameters ω_c, $\lambda/2\omega_0$ and ξ^2 had to be properly chosen, for example, by the method of least squares. These parameters were found to be more or less dependent on the lower frequency at which the measurements had been carried out. From a quantitative coincidence of the experimental data with the calculated data (see figure 3),

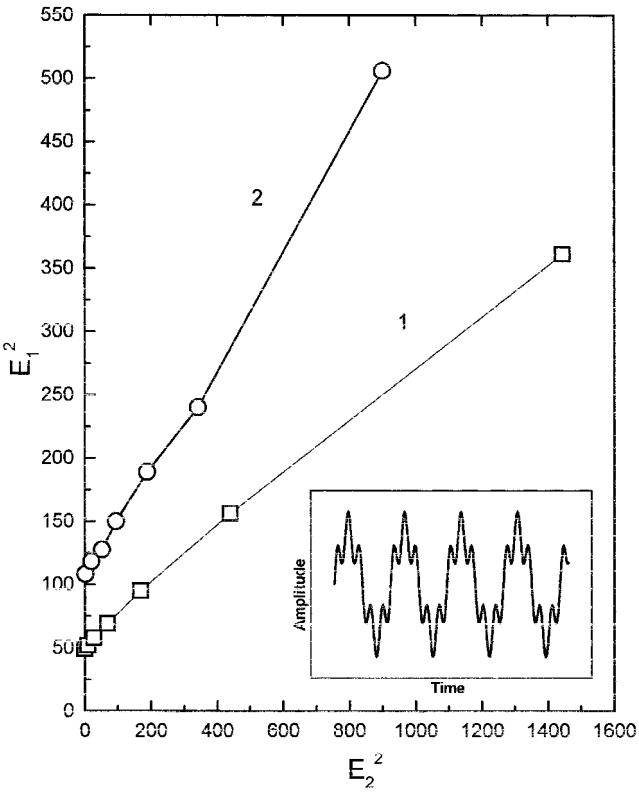

Figure 6. Function dependence between the squares of the amplitudes in the biharmonic field at various frequencies for ZhK-440, $d = 53$ μm. Curve 1: $\omega_1 = 200$ Hz, $\omega_2 = 20$ kHz; curve 2: $\omega_1 = 500$ Hz, $\omega_2 = 20$ kHz.

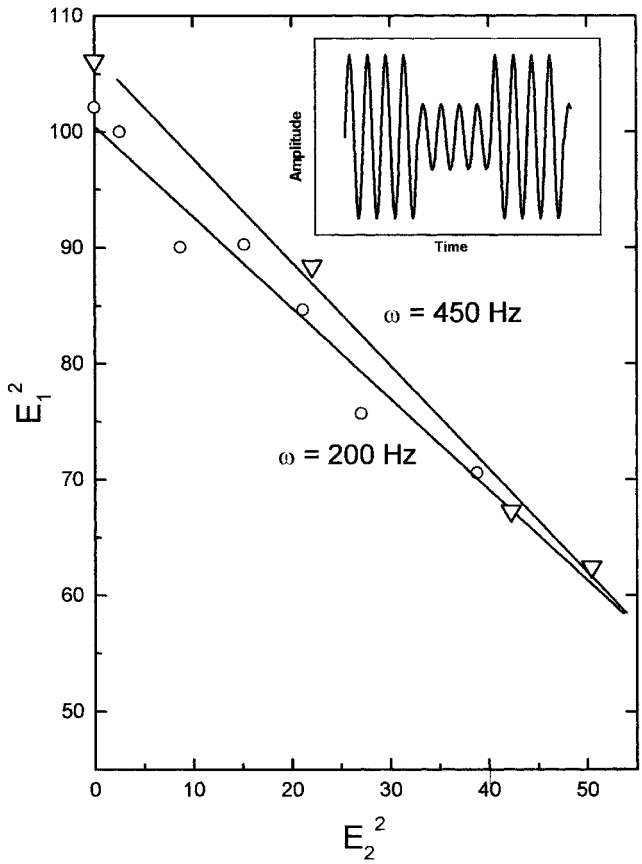

Figure 7. Function dependence between the squares of the amplitudes at different pulse regimes as the frequencies are equal: $T_1 = T_2 = 0.5$ s.

the dependence of some MBBA parameters on the low frequency and temperature are presented in figures 8 and 9, respectively.

The nature of such parameter variations is not quite clear and requires further investigation. However, it is evident that these changes are connected with the dissipative properties of the LC. For instance, it is known [5] that the Leslie coefficients in this frequency range can have a dispersion. It is likely that the abrupt dependence of ξ^2 on temperature, figure 9 (*b*), is mainly due to the change in viscosity since other coefficients entering ξ^2 have only a weak dependence on the temperature under these conditions. In turn, the viscosity is expressed through the Leslie coefficients.

For close frequencies when $\Delta\omega \ll \omega_1, \omega_2$, it is seen from the experimental data presented in figure 4 that the threshold field changes abruptly with the beat period. This behaviour has a clear explanation. Indeed, if $E_0 = E > E_{0c}(E_1 = E_2 = E)$, then in this regime the beating amplitude exceeds the critical value only during some part of the beat period. Depending on this part and the value of E, the instability can (or cannot) have a sufficient time to develop into the observable stage (appearance of diffraction maxima). In figure 4, the values for the threshold voltage corresponding to first occurrence of the diffraction maxima are shown. These values of E_1 are maximum values during the period and can be found from the relation $\gamma T = \pi\omega_0/2\Delta\omega(E_1^2/E_{0c}^2 - 1) = const$ which takes place at the instability onset. Clearly such diffraction patterns will appear and disappear with the beating frequency. It follows from this equation that the critical field depends linearly on $(\Delta\omega)^{1/2}$ as in the case in figure 4. Based on this observation, an express method of determination of the threshold voltage of Williams domains $E(\omega)$ for one frequency ω can be suggested. It is not difficult to obtain

$$E_{0c}^2(\omega) = \left(E_2^2 - E_1^2\frac{\Delta\omega_2}{\Delta\omega_1}\right)\Big/\left(1 - \frac{\Delta\omega_2}{\Delta\omega_1}\right). \qquad (31)$$

Let us choose two values of the frequency difference, for instance, $\Delta\omega_1 = 0.4$ Hz and $\Delta\omega_2 = 0.6$ Hz for $\omega_1 = 200$ Hz. Corresponding values E_1^2 and E_2^2 can be defined from figure 4. Substituting these data in equation (31) gives $V_c(\omega) = E_{0c}d = 9.8$ V which differs from the experimental threshold field for a given frequency ($\Delta\omega = 0$) by

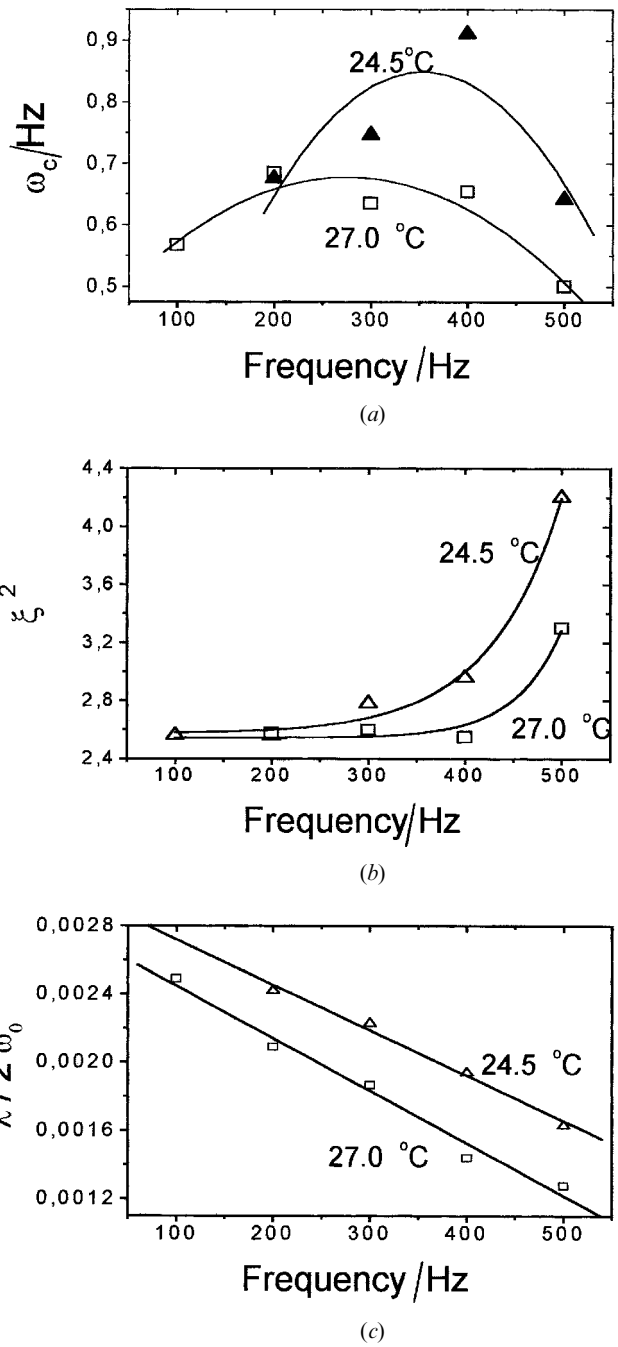

Figure 8. Dependence of MBBA parameters versus low frequency: (*a*) ω_c, (*b*) ξ^2, (*c*) $\lambda/2\omega_0$.

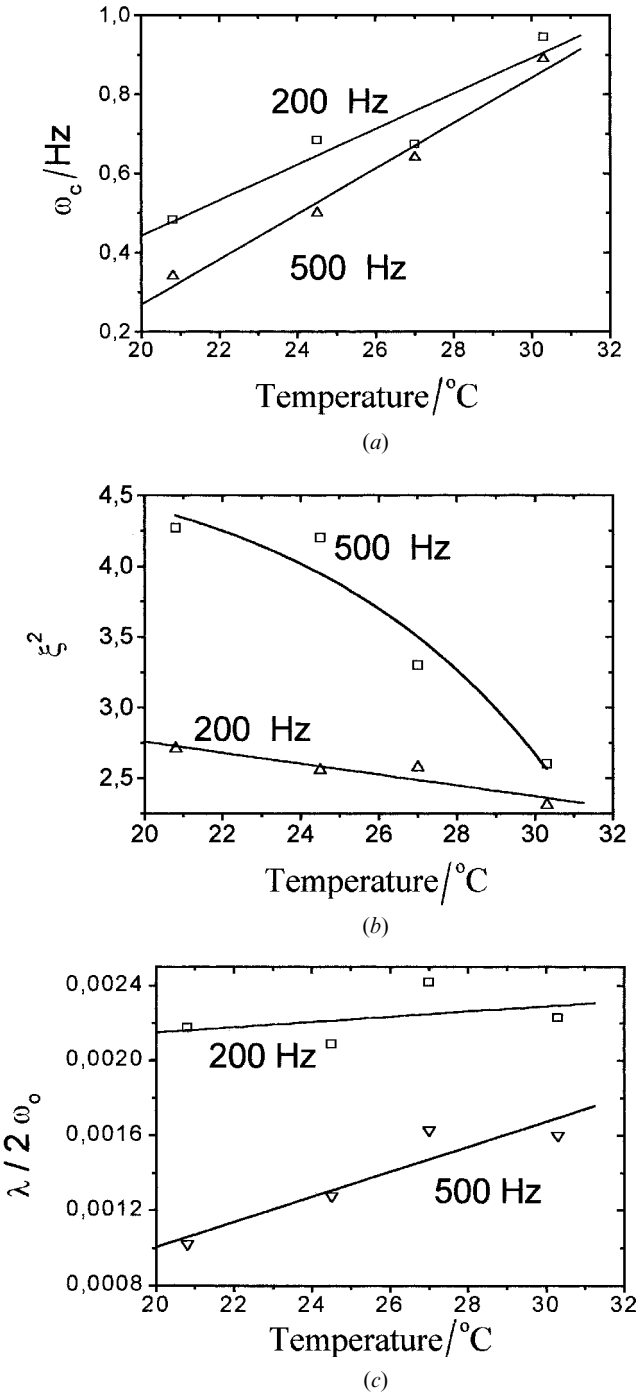

Figure 9. Dependence of MBBA parameters versus temperature: (*a*) ω_c, (*b*) ξ^2, (*c*) $\lambda/2\omega_0$

not more than 10%. Naturally, it is possible to increase the accuracy of determination of the threshold field by accounting for a large number of the beating periods.

Applying the pulsed electric voltage with an amplitude and frequency modulation allows one to study various temporal processes in liquid crystals. The results of our measurement of the Williams domain threshold are shown in figure 5 for an electric field in the form of repeating radio-wave pulses. From equation (29) it is evident that the threshold voltage depends on both times T_2 and T_1. Analysis of experimental data confirms such a dependence. Indeed, at first, the threshold V_c increases with T_2, but then tends to remain constant (for $T_2 > 1.5$ s). The reason for this behaviour is that, on the one hand

the instability—if it occurs within the time of the radio-wave pulse—has a chance to relax to the original state during T_2; on the other hand, V_c is inversely proportional to T_1, and thus decreasing T_1 results in an increase in V_c. The threshold goes up sharply beginning from $T_1 = 0.2 \rightarrow 0.3$ s. It seems likely that the value $0.2 \rightarrow 0.3$ s is the time necessary to develop and visualize Williams domains in the single frequency regime.

Extrapolating T_2 to zero or T_1 to infinity, the values of the threshold field can be obtained in the single frequency regime. Threshold values determined in this way are very close to those measured by the commonly used method. As previously mentioned, the threshold increases in the presence of the high frequency component.

Finally, let us describe the case of amplitude modulation when the patterns relax, not to the original, but to some intermediate state. The experimental result presented in figure 7 corresponds to the case $T_1 = T_2$, $\omega_1 = \omega_2$, and $E_1 \neq E_2$. The instability appears only for definite relations between E_1 and E_2. From figure 7 it is easy to obtain the threshold voltage in the absence of amplitude modulation as determined by the point where $E_1 = E_2$.

We are thankful to O. G. Sarbey and V. M. Pergamenshchik for numerous and useful discussions. B. L. Lev and P. M. Tomchuk gratefully acknowledge financial support by STCU Grant No. 637.

References

[1] De Gennes, P. G., and Prost, J., 1995, *The Physics of Liquid Crystals* (Oxford: Oxford University Press).
[2] Chandrasekhar, S., 1993, *Liquid Crystals* (New York: Cambridge University Press).
[3] Blinov, L. M., 1978, *Electro- and Magneto-Optics of Liquid Crystals* (Moscow: Nauka).
[4] Pikin, S. A., 1978, *Structural Transformation in Liquid Crystals* (Moscow: Nauka).
[5] Kapustin, A. P., 1978, *Experimental investigations of Liquid Crystals* (Moscow: Nauka).
[6] Joest, A., and Ribotta, R., 1986, *J. Phys.*, **47,** 595.
[7] Buka, A., and Kramer, L., editors, 1995, *Pattern Formation in Liquid Crystals* (Berlin: Springer).
[8] Lev, B. I., Sergienko, V. N., Tomchuk, P. M., and Frolova, E. K., 1995, *JETP Lett.*, **62,** 142.
[9] Lev, B. I., Sarbey, O. G., Frolova, E. K., Tomchuk, P. M., and Sergienko, V. N., 1998, *JETP Lett.*, **68,** 881.
[10] Landau, L. D., and Lifshits, E. M., 1973, *Mechanics* (Moscow: Nauka).